

Going beyond an old shockwave conjecture for improving upon Navier-Stokes

Brad Lee Holian^{1,*}, Michel Mareschal^{2,†} and Ramon Ravelo^{1,3,‡}

¹Theoretical Division, Los Alamos National Laboratory, Los Alamos, New Mexico 87545, USA

²Physics Department, Université Libre de Bruxelles, Bld du triomphe, B1050 Brussels, Belgium

³Physics Department, University of Texas at El Paso, El Paso, Texas 79968, USA



(Received 4 October 2023; accepted 2 July 2024; published 24 July 2024)

Nonequilibrium molecular dynamics (NEMD) computer simulations of steady shockwaves in dense fluids and rarefied gases produce detailed shockwave profiles of mechanical and thermal properties. The Boltzmann equation, under the assumption of local thermodynamic equilibrium (LTE), leads to the first-order (linear) continuum theory of hydrodynamic flow: Navier-Stokes-Fourier (NSF). (Expansion of the LTE Boltzmann equation in higher powers of gradients yields so-called Burnett second-order terms, etc.) NEMD simulations of strong shockwaves with high gradients are not well modeled by NSF theory. Many years ago, a conjecture for going “beyond Navier-Stokes” was proposed, applying the empirical observation of anisotropic thermal enhancement in the shock front to the temperature dependence of the NSF transport coefficients, whose dissipation determines the slope at the center of the shock profile: for weak shocks, the actual coefficients in NEMD simulations appear to be smaller than in NSF predictions, leading to steeper gradients being observed, while for strong shocks, the NEMD coefficients appear to be larger, leading to less steep shock rises than predicted by NSF calculations. In this paper, we show that adding significant Burnett nonlinearity into an LTE continuum theory reproduces the early shock rise and slope of NEMD profiles, for both weak and strong shocks in dense fluids, as well as strong shockwaves in the ideal gas. Moreover, we show that “Holian’s conjecture” incorporates significant Burnett nonlinearity, but like all the other LTE continuum theories, it fails to describe the slow NEMD return to equilibrium beyond the shock front. We show that Maxwell relaxation has to be applied to the hydrodynamic variables themselves (rather than attempting indirect relaxation of their gradients) in order to more accurately model the entire shockwave profile. Non-LTE Maxwell relaxation is the only way to bring the entire profile into agreement with NEMD, most noticeably for strong shockwaves.

DOI: [10.1103/PhysRevE.110.015105](https://doi.org/10.1103/PhysRevE.110.015105)

I. INTRODUCTION

In 1970, Alder and Wainwright discovered the hydrodynamic origin of the so-called “long-time tail” of the velocity autocorrelation function using molecular-dynamics (MD) computer experiments [1]. Before A&W’s discovery, it was widely assumed that hydrodynamic behavior could not possibly be seen at such tiny atomistic time and distance scales, much less be able to adequately describe shockwave structure with its enormous gradients of the relevant variables, fluid velocity u , and temperature T . In other words, it would be hopeless to apply first-order (linear in gradients) Navier-Stokes (NS) continuum theory for momentum flux (via the fluid-velocity gradient du/dx) and Fourier’s Law for heat flux (via the thermal gradient dT/dx), in order to compare with nonequilibrium molecular-dynamics (NEMD) simulations of shockwave profiles. Burnett [2] second-order terms, such as the square of the gradients of the hydrodynamic variables, their second derivatives (curvature), and the larger cross term (product of both gradients), were thought to be necessary

additions—at minimum—to NSF hydrodynamics (NSF + B), not to mention including even higher-order (so-called “super-Burnett”) terms. In any event, many theorists even expressed doubts about the convergence of this Taylor serieslike pile on of orders, all of which were fundamentally based upon the notion of “local thermodynamic equilibrium” (LTE), from which the equation of state (EOS) and transport coefficients at zero gradients, obtained from Green-Kubo (G-K) fluctuation-dissipation integrals, could all be computed from equilibrium MD. Later, it was found that computing transport coefficients directly from the ratios of responses to external driving forces by NEMD computer experiments—based on macroscopic hydrodynamic laboratory experiments—was far less computer intensive (even including the slight extra expense of extrapolating to zero gradients), than integrating noisy G-K fluctuations.

In this paper, we recapitulate the history of atomistic simulations of shockwaves [3–5] and their influence upon the development of hydrodynamic (continuum) theory for describing fluid flow, especially since shockwaves probe the challenges of steep gradients in density and temperature [6]. We discuss an old *ad hoc* prescription (“Holian’s conjecture” from several decades ago [7]), an early attempt to improve upon NSF theory, which relies on LTE, in order to predict NEMD shockwave profiles for strong shockwaves. For weak

*Contact author: blhksh@gmail.com; Retired.

†Contact author: michelmaeschal@me.com; Retired.

‡Contact author: ravelo@utep.edu

shockwaves, NSF agrees reasonably well with NEMD simulations, considering the noise level of thermal fluctuations. It is especially for strong shockwaves that the shock rise invokes noticeable nonlinearity, i.e., second-order Burnett terms in density and temperature gradients; moreover, nonequilibrium, i.e., non-LTE, deviations manifest themselves far beyond thermal noise in the relaxation process following the shock front. NEMD provides the exact results toward which continuum theory must strive, and shockwaves provide the most stringent challenge to theory. Holian's conjecture, which incorporates significant Burnett nonlinearity into an LTE continuum treatment by substituting the temperature in the direction of shock propagation, rather than the spatially averaged value, into the NSF transport coefficients' thermal dependence, continues to be tested with limited success, even in recent times. Nevertheless, over a decade ago [8], we found a means to significantly improve agreement with NEMD for the entire shockwave profile, namely, a quantitative linear (exponential) relaxation of the shock front region, using the LTE NSF + B solution as a reference, leading to a full non-LTE hydrodynamic theory.

We will also show how Holian's conjecture relates directly to nonlinear Burnett theory, and yet why all such LTE continuum treatments, by themselves—even though theoretically based upon the generalized Boltzmann's equation,—are incapable of matching NEMD profiles beyond the shock front midpoint.

II. EARLY EFFORTS IN COMPARING CONTINUUM THEORY TO ATOMISTIC COMPUTER EXPERIMENTS

The departure from local thermodynamic equilibrium (LTE) is most pronounced at the midpoint of a planar shockwave in a fluid, which displays noticeable thermal anisotropy [4]. In nonequilibrium atomistic computer simulations (NEMD), the local temperature in a given molecule's neighborhood is measured as thermal fluctuations in molecular velocities relative to the local neighborhood average (fluid velocity) in all three spatial dimensions [9]. In the shockwave direction (x), the longitudinal temperature, T_{xx} , is observed to be higher than the spatial average, T (see Fig. 1). The velocity distribution at the center of the shockwave transforms from an equilibrium spherical gaussian function (Maxwell-Boltzmann) to a nonequilibrium prolate spheroid, whose major axis aligns along the shockwave direction, and which is quantified by a non-Gaussian kurtosis (fourth moment minus three times the square of the second moment) that goes from zero in the initial equilibrium fluid, to positive on the cold side of the shock front, to negative on the hot side, decaying back to zero as the distribution finally returns to equilibrium [4]. Mott-Smith's idea [10] of mixing equilibrium hot and cold (post and preshock equilibrium) Maxwell-Boltzmann distributions in the shockwave was shown to be inconsistent with NEMD profiles, including the erroneous Mott-Smith prediction of a peak in the spatially averaged temperature; in fact, the temperature in the shockwave propagation direction exhibits a peak at the shock front, while the average rises smoothly, as seen in Fig. 1.

A steady planar shockwave in a fluid can be characterized by five hydrodynamic (continuum) local variables:—density ρ , temperature T , fluid velocity in the x -direction u , and

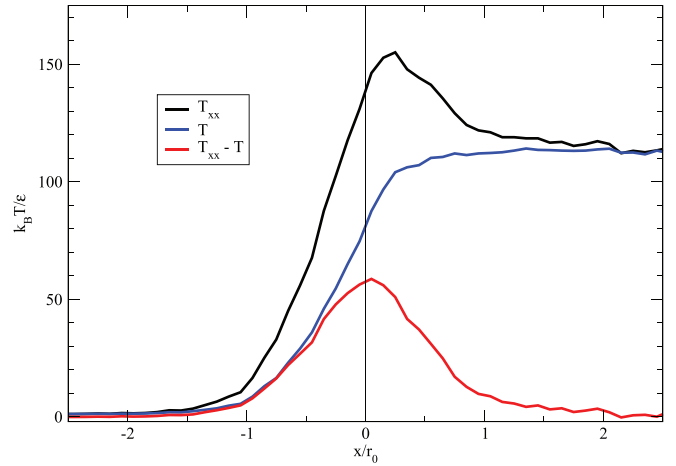


FIG. 1. Nonequilibrium molecular dynamics (NEMD) profiles for a strong steady shockwave in a 3D fluid of atoms interacting via a Lennard-Jones 6-12 pair potential [8,12] (atomic mass = m , equilibrium separation = r_0 , well depth = ϵ), for temperature T , longitudinal temperature T_{xx} , and out-of-equilibrium thermal enhancement ($T_{xx} - T$), in units of temperature ϵ/k_B (k_B is Boltzmann's constant), as functions of the profile position x/r_0 (x is the shock propagation direction) from the shock-front midpoint at $x = 0$, where fluid velocity $u(0) = u_s - u_p/2$ for shock velocity $u_s = 45.2(\epsilon/m)^{1/2}$ (Mach number ≈ 9.3) and piston velocity $u_p = 22.4(\epsilon/m)^{1/2}$; initial density $\rho_0 = 1.0 m/r_0^3$; initial temperature $T_0 = 1.251 \epsilon/k_B$. The curve for the thermal enhancement closely follows the velocity gradient through the profile; see Eq. (1).

zero fluid velocities in the other two transverse directions. By mass conservation, the mass flux ρu is constant, so that the five hydrodynamic variables reduce to two: u and T . For the LTE continuum fluid-flow theory, NSF + B—linear Navier-Stokes-Fourier, plus a nonlinear (quadratic) Burnett modification of the heat flux, where the thermal gradient (dT/dx) is multiplied by the fluid-velocity gradient (du/dx),—the anisotropic enhancement of the temperature in the direction of a planar shockwave ($T_{xx} - T$) can be approximated [8] from the pressure tensor components by

$$T_{xx} - T \cong \left(\frac{\partial T}{\partial P} \right)_\rho \cdot (P_{xx} - P) = \left(\frac{\partial T}{\partial P} \right)_\rho \left(-\eta_L \frac{du}{dx} \right) \geq 0, \quad (1)$$

where P_{xx} is the Navier-Stokes momentum flux (longitudinal pressure), given by

$$P_{xx} = P(x) - \eta_L(x) \frac{du}{dx}. \quad (2)$$

The shock profile coordinate (in the propagation direction) is x ; η_L is the longitudinal viscosity, a sum of bulk η_V and shear η_S viscosities: $\eta_L = \eta_V + (4/3)\eta_S$.

For the ideal gas, Eq. (1) is an identity; otherwise, we must emphasize that T_{xx} can be measured only in NEMD simulations;—in other words, T_{xx} is beyond the scope of continuum theory for dense fluids [4]. The fluid-velocity gradient is negative at the steady shockwave center ($x = 0$), since the cold fluid coming from the left at velocity u_s stagnates against a piston moving off to the right at $u_s - u_p$. In the laboratory frame, u_s is the shock velocity produced when an

infinitely massive piston collides with a stationary sample at the piston velocity u_p . For NSF theory, the EOS (equilibrium equation of state: pressure P and internal energy E) and the set of (positive) transport coefficients (bulk and shear viscosities for Navier-Stokes fluid flow and thermal conductivity for Fourier's heat flow) are functions of density ρ and temperature T , evaluated at the shock profile coordinate, x .

The first NEMD simulations of a weak planar shockwave in a dense Lennard-Jones fluid were performed in 1978 by Klimenko and Dremin [3]. In 1979, Hoover proposed comparing their NEMD results with NSF continuum theory, which showed remarkable agreement with the atomistic results, despite the previously assumed inapplicability of NSF at such small time and distance scales as exist at shock fronts [6]. The NEMD weak-shock profiles were observed to be somewhat steeper than calculated from continuum theory.

Soon thereafter, in 1980, Holian *et al.* performed NEMD simulations of a much stronger shockwave in the same Lennard-Jones fluid [4], to see if notable differences could be seen between NEMD and the NSF continuum prediction. In this case, which more closely approaches the ideal gas limit at the middle of the shock front, the NEMD profiles were noticeably broader than calculated by NSF. The paper contains nonequilibrium details (i.e., beyond NSF theory) about the anisotropy of the velocity distribution, as well as methodology on how to sample slabs of atoms in the shockwave propagation direction, in order to correct the measured shock thickness for bin size. (Notably, they showed that shock thickness is never as narrow as one mean free path; it is always a handful.)

The authors made the following noteworthy statement in their paper: "There is no reason why a linear theory describing the decay of differences between longitudinal and transverse temperatures could not be developed." And then they concluded by saying, "Theoretical efforts to go beyond the Navier-Stokes level have not been completed yet." Going "beyond Navier-Stokes" with a deeper understanding of the fundamental physics of fluids and gases would take the fullness of time—another three decades [8,11,12].

A 1988 paper, entitled "Modeling of shockwave deformation by molecular dynamics," summarized the NEMD fluid shockwave work up to that time [7]. For the temperature dependence of the longitudinal viscosity and thermal conductivity at the middle of the shock front—in NSF theory, the determinants of the steepness of shock profile gradients,—one might be tempted to take advantage of the thermal enhancement ($T_{xx} \geq T$) of the longitudinal temperature in the shock direction over the spatially averaged temperature. In the weak-shock case, if the dense fluid's viscosity were to depend on T_{xx} , rather than T , it would be lower (warming up your honey makes it flow more easily), and the resulting modified NSF profile of u (similar for conductivity and the NSF profile of T) would thus be steeper and narrower, in agreement with NEMD results. In the strong-shock case, with temperature high enough to approach ideal-gas behavior, if the viscosity and conductivity were to depend on T_{xx} , rather than T , they would be higher (contrary to dense-fluid behavior), making the modified NSF theory's shock rise in profiles less steep and the shock thickness broader, in agreement with NEMD. In other words, the density and temperature dependence of

the NSF transport coefficients could, conceivably, be modified and therefore better represented by T_{xx} , rather than T , for both weak and strong shockwaves. NEMD shockwave simulations for the ideal gas and NSF continuum comparisons, including replacement of T by T_{xx} in the transport coefficients' temperature dependence (so-called "Holian's conjecture"), reinforced the empirical dense-fluid observations [13].

We note here—that Eq. (1) shows how replacing T by T_{xx} in the thermal conductivity's temperature dependence introduces the velocity gradient into the NSF heat flux, thereby mimicking the second-order Burnett term in NSF + B; of course, Holian's conjecture also introduces the second power of velocity gradient into the momentum flux. (See the Appendix for details of Holian's conjecture's relationship to Burnett theory). While improving the gradients' slopes at the shock front, Holian's conjecture, like other LTE continuum theories, cannot reproduce the slow return to post-shock equilibrium, as seen on the hot side of NEMD profiles. After the 1993 strong-shock ideal-gas paper, a number of authors began testing Holian's conjecture for weaker ideal-gas shockwaves with limited success [14], and have continued their efforts over the years, until even quite recently [15–22]. The limitations of LTE continuum theories of all kinds are manifest in poor agreement with post-shock recovery of equilibrium: NEMD always takes a leisurely pace compared to predictions.

III. RECENT ADVANCES IN HYDRODYNAMIC THEORY

In a series of papers [8,11,12] Holian, Mareschal, and Ravelo demonstrated that the shock profiles, for both the ideal gas and dense fluids, could finally best be understood as systems driven out of local equilibrium, producing thermal anisotropy in the shock front, followed by relaxation back to local thermodynamic equilibrium. The reference LTE continuum solution can be solved by step-wise (Δx) integration through the shock profile coordinate x , starting at the hot, compressed side and moving toward the cold, for the NSF + B hydrodynamic variables u_{ref} (fluid velocity) and T_{ref} (average temperature). The exponential relaxation equation, in the spirit of Maxwell and Cattaneo, for T (similarly for u) is given by

$$T' = \frac{dT}{dx} = -\frac{T - T_{\text{ref}}}{\lambda}. \quad (3)$$

Cattaneo was inspired, nearly a century after Maxwell, to add relaxation of the heat flux to Fourier's Law of heat flow [23], in much the same spirit that Maxwell's viscoelasticity model relaxes momentum flux (Navier-Stokes stress). In Maxwell's model of viscoelasticity, the total strain rate is proportional to the elastic and viscous strain:

$$\eta \frac{d\varepsilon}{dt} = \sigma + \frac{\eta}{B} \frac{d\sigma}{dt}, \quad (4)$$

where stress is σ , strain is ε , viscosity is η , and elastic modulus is B . Defining a relaxation time $\tau = \eta/B$ and viscous stress $\sigma_{\text{ref}} = \eta d\varepsilon/dt$, the canonical exponential relaxation can be expressed as

$$\frac{d\sigma}{dt} = -\frac{\sigma - \sigma_{\text{ref}}}{\tau}. \quad (5)$$

Our approach differs from Maxwell and Cattaneo in relaxing the NSF + B hydrodynamic variables u_{ref} and T_{ref} themselves, rather than relaxing the heat flux, a quadratic function of fluid velocity, and a hard-to-untangle function of temperature from the internal energy; on the other hand, relaxing the longitudinal pressure, the momentum flux, is equivalent to relaxing the fluid velocity, since they are linearly related. The profile of u_{ref} exhibits a symmetrical shape like the hyperbolic tangent; density ρ is derived from it, since the mass flux in the planar, steady shock is a constant. In our relaxation equation (above), the mean free path λ is the product of sound velocity c and the local thermodynamic mean collision time τ , as computed from the EOS at the shockwave center. The observed shockwave thickness is just a few mean free paths, making a connection between atomistic simulations and continuum theory plausible, contrary to previously accepted “wisdom.” The mean free path λ and collision time τ can be expressed in terms of the speed of sound c , density ρ , bulk modulus B , and kinematic viscosity η_L/ρ as

$$\lambda = c\tau, \quad \tau = \frac{\eta_L}{B}, \quad B = \rho c^2, \quad c^2\tau = \frac{\lambda^2}{\tau} = \frac{\eta_L}{\rho}. \quad (6)$$

The Fourier heat flux, multiplied by the largest and most significant nonlinear Burnett correction (product of velocity and temperature gradients, with dimensionless parameter δ), is given by

$$Q(x) = -\kappa(x) \left[1 - \delta \cdot \tau(0) \frac{du}{dx} \right] \frac{dT}{dx}, \quad (7)$$

where κ is the thermal conductivity. For the ideal gas shockwave, the dimensionless parameter $\delta = 3.6$ can be computed from Burnett equations [5] using Chang and Uhlenbeck’s kinetic theory for hard spheres [24]; for molecules interacting by a repulsive potential with the inverse fourth power of distance (so-called Maxwell molecules), $\delta = 4.25$; for repulsions steeper than inverse fourth power, such as inverse twelfth (so-called “soft spheres”), the results fall systematically in between these two limits. For the strong shockwave in the Lennard-Jones dense fluid, no Burnett kinetic theory calculations have been done, so we have simply used the hard-sphere ideal-gas parameter for our continuum NSF + B comparisons to NEMD; for weak shocks, transport coefficients decrease with temperature, so that δ is negative in that case. However, we warn readers that arbitrarily setting the NSF + B δ to a large enough negative number in the calculation could cause heat to flow against the temperature gradient, i.e., from the cold side of the shockwave toward the hot,—an unphysical catastrophe [18], indeed.

The relaxation, accompanying each step in the NSF + B integration, employs the central difference approximation, which is shown here for the relaxed T (similarly for u):

$$T(x + \Delta x) = \frac{1}{1 + \frac{\Delta x}{2\lambda}} \left\{ T(x) \cdot \left[1 - \frac{\Delta x}{2\lambda} \right] + [T_{\text{ref}}(x) + T_{\text{ref}}(x + \Delta x)] \cdot \frac{\Delta x}{2\lambda} \right\} + \mathcal{O}(\Delta x^3). \quad (8)$$

Figure 2 shows the longitudinal pressure profile and its deviation from isotropic pressure ($P_{xx} - P$) for a strong shockwave in the Lennard-Jones dense fluid. The resulting

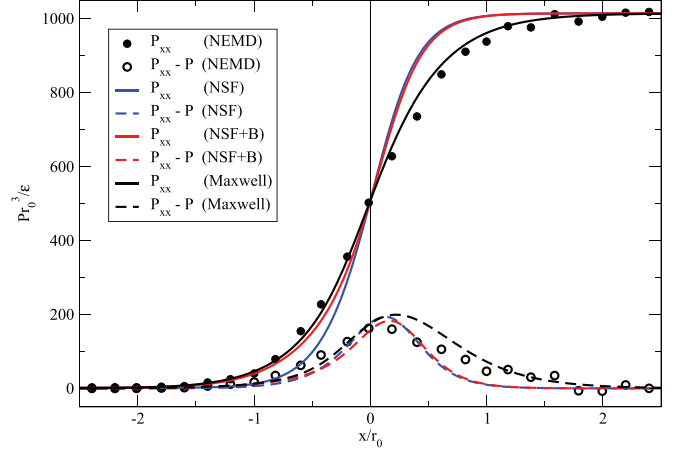


FIG. 2. NEMD shockwave profiles of longitudinal pressure P_{xx} and pressure difference ($P_{xx} - P$) in pressure units of ϵ/r_0^3 for a strong shock in a dense Lennard-Jones fluid (see Fig. 1 caption). Exact (atomistic) results are compared to continuum theories: linear Navier-Stokes-Fourier (NSF), nonlinear Burnett (NSF + B), and linear (exponential) relaxation applied to NSF + B solution (Maxwell). Note that, as predicted by non-LTE Maxwell relaxation, NEMD returns more slowly to the final equilibrium state than any of the LTE continuum theories.

comparison between NEMD and this relaxed continuum treatment is almost quantitative; in the same paper, we also showed quantitative agreement for a strong shockwave in the ideal gas (Fig. 3) [8]. The early shock rise is better represented by the nonlinear Burnett correction to the heat flow (NSF + B) than the NSF prediction by itself [11,12] but the slower

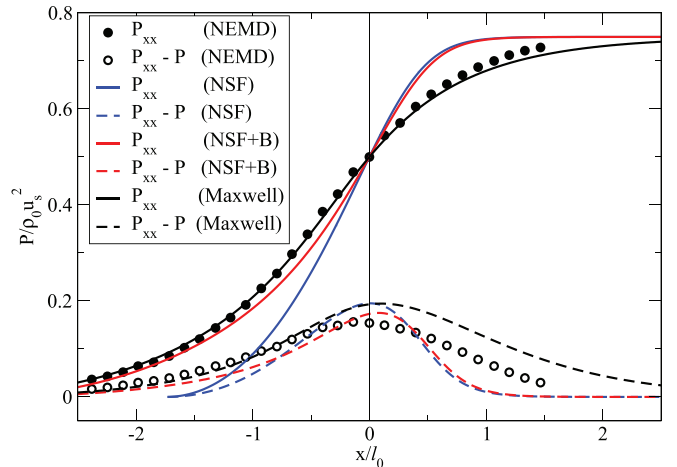


FIG. 3. Shockwave profiles of longitudinal pressure P_{xx} and pressure difference ($P_{xx} - P$) for a strong shock in an ideal gas (Mach number = $u_s/c_0 = 134$, where c_0 is the bulk sound speed of the initial state); exact atomistic results (NEMD) [5] are compared to continuum theories [8]: linear Navier-Stokes-Fourier (NSF), nonlinear Burnett (NSF + B), and linear (exponential) relaxation applied to NSF + B solution (Maxwell). The x position is scaled by the mean free path in the initial cold state, l_0 . As in dense fluid shockwaves, linear relaxation of the best continuum solution (NSF + B) is required to match NEMD’s slower return to the post-shock equilibrium state.

decay back to LTE that is observed in NEMD profiles requires exponential relaxation of the NSF + B variables (in the spirit of Maxwell-Cattaneo) [8]. We emphasize that our approach is beyond the reach of the LTE Boltzmann equation, in that relaxation from non-equilibrium conditions in the shockwave front is performed upon the entire LTE continuum reference solution; it is therefore a novel departure from all past efforts to go beyond Navier-Stokes [13–22].

IV. CONCLUSION

The historical path for going “beyond Navier-Stokes” is a long and winding road, full of discoveries and notable improvements in our understanding. Local thermodynamic equilibrium has had a long history, and the shockwave has shown just how violation of LTE can be recovered in a predictable way—beyond any *ad hoc* conjectures.

The first clue to convergence in the Taylor-series orders of continuum hydrodynamical theory was the level of agreement between NEMD shockwave profiles (i.e., the exact classical-mechanical results) for dense fluids and dilute gases with NSF. The second clue was employing the largest Burnett cross-term of gradients (NSF + B) for improving the profiles of u and T , at least up to the midpoint of the shock front, where both gradients reach a maximum. Higher-order terms appeared to make no significant improvement: thus, the limit of LTE had apparently been reached.

The final resolution for hydrodynamic theory was to apply Maxwell-Cattaneo exponential relaxation directly to the hydrodynamical field variables (u and T) themselves. That is to say, the NSF + B LTE solutions, which drive the system to a nonequilibrium condition ($P_{xx} > P$) in the middle of the shock front, were used as the reference state for the relaxation back to LTE, as seen in the exact NEMD profiles [8].

What remains to be done for the future improvements to hydrodynamic theory? Our NSF + B solutions for u and T , and the EOS and transport coefficients for both the fluid and gas we studied, involved fits to MD and NEMD data at the zero-gradient Green-Kubo limit—a potential source of relatively tiny errors. The Maxwell-Cattaneo exponential relaxation we carried out on the NSF + B (LTE) continuum solution assumed a constant relaxation length λ (mean free path), evaluated at $x = 0$. Instead, a better approach might be to assume that λ is computed locally at each point x along the shock profile. This might resolve the small remaining discrepancies between our continuum approach and the NEMD shock profiles. The major improvements made in our understanding of hydrodynamics a decade ago [8] have led us to re-evaluate the provisional *ad hoc* prescription, “Holian’s conjecture [7]. We now recognize that this conjecture,—replacing T with T_{xx} in the NSF transport coefficients,—modifies the NSF solution to incorporate significant Burnett nonlinearity, and since there is no adjustable parameter (such as the temperature-dependent NSF + B δ), it is therefore a viable candidate for future work as a reference solution for applying our method of Maxwell-Cattaneo relaxation back to LTE. Without relaxation, Holian’s conjecture suffers the same difficulty as all other LTE continuum theories in comparison to NEMD shockwave profiles: NEMD takes considerably longer to get back to equilibrium.

Finally, the domain of non-LTE behavior is clearly a rather narrow zone, namely, the thickness of the shock front,—a handful of mean free paths, — nanometers in strong shockwaves, rather than millimeters.

ACKNOWLEDGMENTS

Part of this work was supported by Los Alamos National Laboratory under US Department of Energy Contract No. 89233218CNA000001.

APPENDIX: BURNETT NONLINEARITY OF HOLIAN’S CONJECTURE

In this Appendix, we show that Holian’s conjecture exhibits Burnett nonlinearity. Whereas our previous papers introduced Burnett nonlinearity into the heat flux only [Eq. (5)], Holian’s conjecture also applies to the momentum flux [Eq. (2)].

Holian’s conjecture can be formulated as replacing the temperature dependence on the spatially averaged temperature T by the temperature in the shockwave direction T_{xx} , for both the longitudinal viscosity and thermal conductivity:

$$\eta_L^{(0)} = \eta_L(\rho, T), \quad \eta_L^{(1)} = \eta_L(\rho, T_{xx}), \quad (\text{A1})$$

$$\kappa^{(0)} = \kappa(\rho, T), \quad \kappa^{(1)} = \kappa(\rho, T_{xx}). \quad (\text{A2})$$

Beginning with the anisotropic temperature enhancement [Eq. (1)], where $\Delta T = T_{xx} - T$ and $(x) \Rightarrow (\rho, T)$,

$$\Delta T = -\frac{BV}{\gamma C_V} \cdot \tau \frac{du}{dx}, \quad (\text{A3})$$

where the Grüneisen parameter $\gamma = V(\partial P/\partial E)_V$, the constant-volume heat capacity $C_V = (\partial E/\partial T)_V$, the collision time from Eq. (4) $\tau = \eta_L^{(0)}/B$, and volume V (containing N atoms of atomic mass m) is determined from the mass density $\rho = Nm/V$.

For example, the longitudinal viscosity can be expanded in powers of ΔT (thermal conductivity is analogous):

$$\eta_L^{(1)} = \eta_L^{(0)} + \frac{d\eta_L^{(0)}}{dT} \Delta T + \mathcal{O}(\Delta T)^2 \quad (\text{A4})$$

$$= \eta_L^{(0)} \left[1 - \frac{BV}{\gamma C_V} \left(\frac{1}{\eta_L^{(0)}} \frac{d\eta_L^{(0)}}{dT} \right) \cdot \tau \frac{du}{dx} \right] + \mathcal{O}(du/dx)^2. \quad (\text{A5})$$

We can define a dimensionless parameter δ_u for the fluid velocity u :

$$\delta_u = \frac{BV}{\gamma C_V} \frac{d \ln(\eta_L^{(0)})}{dT}, \quad (\text{A6})$$

whence the Navier-Stokes momentum-flux equation [Eq. (2)] becomes

$$P_{xx} - P = -\eta_L^{(1)} \frac{du}{dx} = -\eta_L^{(0)} \left(1 - \delta_u \cdot \tau \frac{du}{dx} \right) \frac{du}{dx} + \dots \quad (\text{A7})$$

For the temperature T , a dimensionless parameter δ_T is defined by

$$\delta_T = \frac{BV}{\gamma C_V} \frac{d \ln(\kappa^{(0)})}{dT}, \quad (\text{A8})$$

so that the Fourier heat-flux equation [Eq. (5)] becomes

$$Q = -\kappa^{(1)} \frac{dT}{dx} = -\kappa^{(0)} \left(1 - \delta_T \cdot \tau \frac{du}{dx} \right) \frac{dT}{dx} + \dots \quad (\text{A9})$$

Therefore, Holian's conjecture includes major second-order nonlinear Burnett terms in both u and T , apart from a quadratic temperature gradient. Also, curvature in either of the two hydrodynamic fields is neglected—these are nearly zero at the shock front, where the gradients are linear. Despite giving better agreement with NEMD shock profiles in the early rise, Holian's conjecture shares a failing with all continuum theories based on local thermodynamic equilibrium, namely, a too-rapid return to the final equilibrium state for collision times following the midpoint of the shock front.

-
- [1] B. J. Alder and T. E. Wainwright, *Phys. Rev. A* **1**, 18 (1970); see historical details and modern perspective in B. L. Holian, *Eur. Phys. J. H* **46**, 1 (2021).
- [2] D. Burnett, *Proc. London Math. Soc.* **s2-40**, 382 (1936).
- [3] V. Y. Klimenko and A. N. Dremin, in *Detonatsiya Chernogolovka*, edited by O. N. Breusov *et al.* (Akademik Nauk, Moscow, 1978), p. 79.
- [4] B. L. Holian, W. G. Hoover, B. Moran, and G. K. Straub, *Phys. Rev. A* **22**, 2798 (1980).
- [5] E. Salomons and M. Mareschal, *Phys. Rev. Lett.* **69**, 269 (1992).
- [6] W. G. Hoover, *Phys. Rev. Lett.* **42**, 1531 (1979).
- [7] B. L. Holian, *Phys. Rev. A* **37**, 2562 (1988).
- [8] B. L. Holian, M. Mareschal, and R. Ravelo, *Phys. Rev. E* **83**, 026703 (2011).
- [9] J. H. Irving and J. G. Kirkwood, *J. Chem. Phys.* **18**, 817 (1950); Irving and Kirkwood derived expressions in terms of atomic coordinates and momenta for Navier-Stokes momentum flux (the pressure tensor) and Fourier heat flux that have been used for well over 50 years in the analysis of molecular-dynamics computer simulations.
- [10] H. M. Mott-Smith, *Phys. Rev.* **82**, 885 (1951).
- [11] B. L. Holian and M. Mareschal, *Phys. Rev. E* **82**, 026707 (2010).
- [12] B. L. Holian, M. Mareschal, and R. Ravelo, *J. Chem. Phys.* **133**, 114502 (2010).
- [13] B. L. Holian, C. W. Patterson, M. Mareschal, and E. Salomons, *Phys. Rev. E* **47**, R24 (1993).
- [14] M. López de Haro and V. Garzó, *Phys. Rev. E* **52**, 5688 (1995).
- [15] F. J. Uribe, R. M. Velasco, and L. S. García-Colín, *Phys. Rev. E* **58**, 3209 (1998).
- [16] D. Jou, J. Casas-Vázquez, and G. Lebon, *Rep. Prog. Phys.* **62**, 1035 (1999).
- [17] Y.-G. He, X.-Z. Tang, and Y.-K. Pu, *Phys. Rev. E* **78**, 017301 (2008).
- [18] F. J. Uribe, W. G. Hoover, and C. G. Hoover, *CMST* **19**, 5 (2013).
- [19] F. J. Uribe, *Phys. Rev. E* **93**, 033110 (2016).
- [20] R. S. Jadhav and A. Agrawal, *Phys. Rev. E* **102**, 063111 (2020).
- [21] R. S. Jadhav and A. Agrawal, *Fluids* **6**, 427 (2021).
- [22] R. M. Velasco and F. J. Uribe, *Wave Motion* **100**, 102684 (2021).
- [23] C. Cattaneo, Sulla Conduzione Del Calore, in *Some Aspects of Diffusion Theory*, edited by A. Pignedoli, Vol. 42 (C.I.M.E. Summer Schools, Springer, Berlin, Heidelberg, 2011), p. 485.
- [24] C. S. Wang Chang and G. E. Uhlenbeck, in *Studies in Statistical Mechanics*, edited by J. de Boer and G. E. Uhlenbeck (North-Holland, Amsterdam, 1970), Vol. 5, pp. 8-10.